Low Cost, Good Accuracy - Attitude Determination Using Magnetometer and Simple Sun Sensor

Stephan Theil, Pontus Appel, Alexander Schleicher

Center of Applied Space Technology and Microgravity (ZARM), University of Bremen,
Am Fallturm, D-28359 Bremen, Germany, Phone: +49-421-2183551,
E-mail: theil@zarm.uni-bremen.de

Abstract

A low cost, robust Attitude Determination System with good accuracy for small satellites can be achieved by using a combination of magnetometer and Coarse Sun Sensor. The Coarse Sun Sensor consists of solar cells placed on each of the six outside surfaces of the satellite. The main measurement error of the Coarse Sun Sensor occurs due to the Earth's albedo which can cause an angular deviation of more than 20 degrees. By modeling the albedo and applying state estimation methods for attitude determination the error can be reduced drastically to less than 1 degree, depending on the conditions.
In the first part of this paper the development of the albedo model is presented. It is used to correct the measurements of the Coarse Sun Sensor as well as to have a realistic simulation of the sensor. The albedo model of the Earth is created using existing reflectivity data. The variation of the reflectivity is analyzed statistically and parametric functions are derived to describe the albedo light vector received by a satellite in its orbit.
In the second part an Extended Kalman Filter for attitude determination is presented which is using the two vectors provided by the magnetometer and the Coarse Sun Sensor. A model of the total light vector - the sum of sunlight and Earth albedo light - and the magnetic field vector taken from the IGRF model are utilized as the measurement model. The paper will present simulation results showing the accuracy of the attitude determination system for various types of orbits.

Introduction

For most small satellite applications a moderate pointing accuracy of about 1 degree in all axes is sufficient. This is usually achieved by two sets of sensors. One set is utilized for attitude acquisition. The second is used for the nominal mission. The more the two sets overlap the larger is the benefit in saving costs, space and mass. So the objective should be the utilization of one set of sensors only for the whole mission. On one hand these sensors must be robust for the attitude acquisition phase. On the other hand they have to provide the required accuracy. The latter can be achieved using low cost, low accuracy sensors and intelligent algorithms to improve the capabilities of the attitude determination system.
One very reliable and simple possibility to combine low cost, robust sensors for attitude determination of small satellites is the combination of a magnetometer and a Coarse Sun Sensor. The Coarse Sun Sensor is a simple sensor consisting of six solar cells placed on each of the six outside surfaces of the satellite. It delivers basically the light vector - assumed to be the vector to the Sun - in satellite body-fixed coordinates. The main measurement error of the Coarse Sun Sensor occurs due to the Earth's albedo which can cause an angular deviation of the Sun vector by more than 20 degrees. By modeling the albedo and applying state estimation methods for attitude determination the error can be reduced drastically to less than 1 degree, depending on the conditions.

This paper introduces the simple Coarse Sun Sensor (CSS) and describes a model for the albedo light in order to compensate for this systematic error source. In the second part an Extended Kalman Filter is presented which applies the albedo model for attitude estimation improvement.

The Coarse Sun Sensor

The Coarse Sun Sensor (CSS) consists of six solar cells placed on each of the outside surfaces of the satellite. Using the cosine law the amount of incoming light can be calculated for each cell and so the angle towards the Sun. Figure 1 shows one sensor head of a CSS. It has two redundant solar cells ($24 \times 24mm$) as main detector. The size of the surface area is $27mm \times 54mm$.

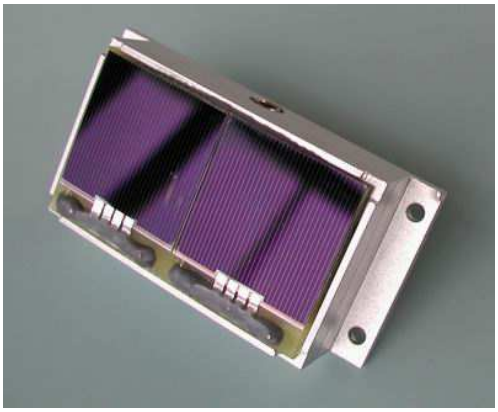

Figure 1: Single Coarse Sun Sensor Head.

Figure 2 describes one way to place the cells on a cubic satellite. The cells should be placed where the risk of being shaded by other objects is negligible. The coordinate system used for determination of the direction of the solar cell surface normal is a body-fixed one.

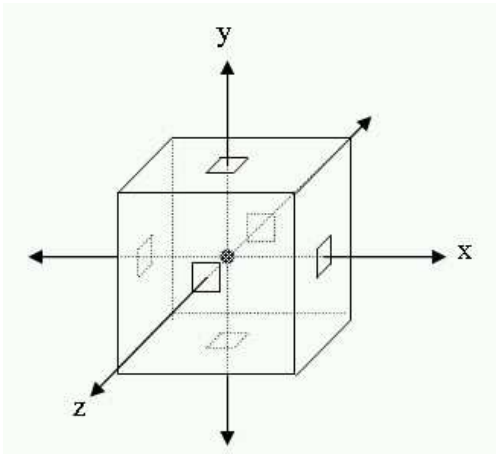

Figure 2: Orientation of the 6 heads of a CSS.

The solar cell delivers a voltage that is proportional to the incoming light. The amplitude of the voltage follows the cosine law. With tests the characteristics of the cell were examined. Figure 3 shows the results from these tests.

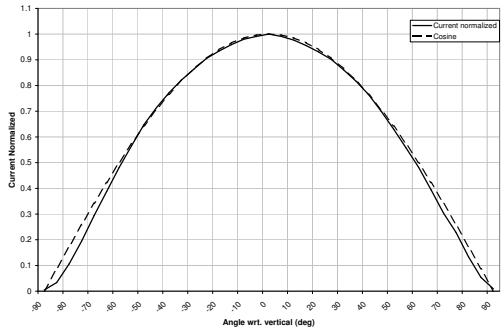

Figure 3: Current produced by a solar cell vs angle of light incident.

The figure shows the resulting normalized current through a resistor connected to the cell as a function of the angle of the incoming light. The solid lower curve represents the test results and the dashed upper one is a cosine curve. The results show that the modeling of the delivered voltage from the cell can be done with a simple cosine function.
If the deviation from the cosine function is small the raw measurements can be used to obtain the direction of the total incoming light vector. The unit vector in this direction can be derived as

$$\underline{e}^b_{total} = \frac{1}{I_{total}} \begin{bmatrix} I_{+X} - I_{-X} \\ I_{+Y} - I_{-Y} \\ I_{+Z} - I_{-Z} \end{bmatrix} \tag{1}$$

where

$$\begin{aligned} I^2_{total} = &(I_{+X} - I_{-X})^2 + \\ &(I_{+Y} - I_{-Y})^2 + \\ &(I_{+Z} - I_{-Z})^2 \end{aligned} \tag{2}$$

and I_{+X} is the current produced by the solar cell sensor head in X-direction. Analogously the other directions are named.
If the solar cells presented are placed as indicated they can together deliver the direction of an incoming light vector when using the right interpreter. The accuracy of the direction determination is good and the costs much lower than when using a normal fine sun sensor. The sensors are also reliable because of their simple construction. As a complement or substitute to the small sensors the ordinary solar cells of a satellite can be used.

Albedo Model

As the CSS, unlike a fine Sun sensor, sees the whole sky it is much more sensitive to other light sources than the Sun. The largest of these sources for a satellite in a low Earth orbit is the light reflected by Earth, the Earth albedo. To be able to get a good estimation of the Sun vector the Earth albedo has to be compensated. This can

be done by developing an albedo model and including it in the attitude estimation algorithm.
In order to calculate the amount of light received by a satellite in orbit a model for the light reflected by Earth is needed. The incoming light is a function of the satellite position, the position of the Sun and the reflectivity of the Earth. In the model it is assumed that the Earth emits the radiation like a black body. Therefore the main part of the light is assumed to be reflected by the Earth diffusely. The radiation from a black body is isotropic. Therefore it has no preferred direction. In this case the Lambertian cosine law is applicable.

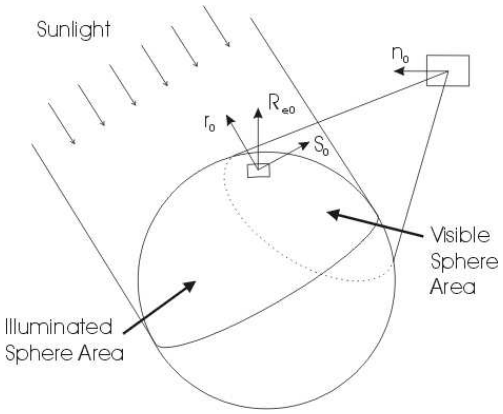

Figure 4: Geometry of the albedo light incident on a satellite.

As the incoming sunlight hits the Earth it is diffusely reflected by the atmosphere and Earth surface in all directions. The amount of emitted light is determined by the reflectivity of the element and the angle of the incoming light. The amount of emitted light in the direction of the satellite is decided by the angle between the surface element normal and the satellite vector. The voltage delivered by the solar cell receiving the light is also calculated with the cosine law with the satellite vector and solar cell surface normal as components. The path of the light and the vectors are described in Figure 4 The amount of incoming light to the satellite is equal to the integral of three vector products over the illuminated and visible area of Earth. The total received energy is

$$\dot{Q} = \frac{I_s A_{cell}}{\pi} \iint\limits_{A_{vis,il}} \frac{\rho \left(\underline{R}_{e,0} \circ \underline{S}_0\right) \left(\underline{S}_0 \circ \underline{n}_0\right) \left(\underline{R}_{e,0} \circ \underline{r}_0\right)}{S^2} \mathrm{d}A \tag{3}$$

where

I_s	Solar light intensity at Earth.
A_{cell}	Solar cell surface area.
ρ	Reflectivity of the surface element of the Earth.
$\underline{R}_{e,0}$	Surface element normal vector.
$\underline{S}_0$	Vector pointing from surface element to the satellite.
$\underline{n}_0$	Solar cell normal vector.
$\underline{r}_0$	Vector pointing to the Sun.

The solution of Equation 3 is needed for every point in the orbit of a satellite. Because of its complexity with the non-trivial limits of integration it can not be solved analytically. Together with the fact that the reflectivity of Earth is far from being uniform this implies that a numerical solution is the best way to solve the problem.

Reflectivity Model and Reflectivity Data

First a numerical model of the Earth is created by dividing a sphere into a finite number of surface elements. A reflectivity model is developed to describe the reflectivity of every single element.
To get a realistic reflectivity distribution reflectivity data from existing measurements is analyzed. The data is taken from the NASA project Total Ozone Mapping Spectrometer (TOMS).[2] Plotting the data shows Earth's reflectivity as a function of the latitude and longitude. Figure 5 shows the reflectivity reading from one day.

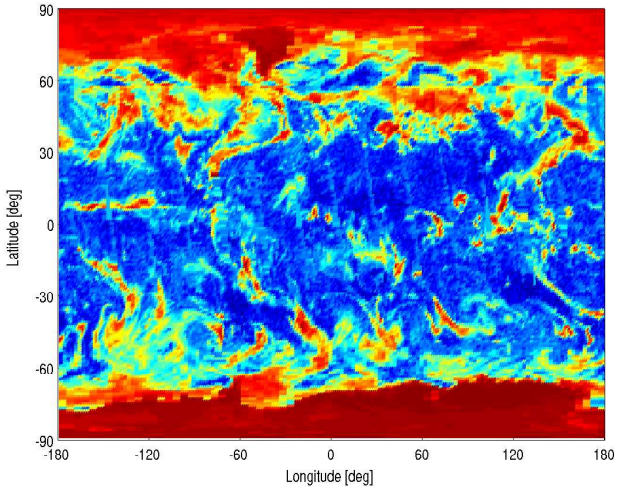

Figure 5: Daily reflectivity data of the Earth.[2]

The bright areas represent high reflectivity and the dark areas represent low reflectivity. From the plot the polar regions and Greenland (latitude $-40\,deg$, longitude $+60\,deg$) can be recognized as well as several cloud formations. It can be seen that a lot of the reflected light

origins from these cloud formations and the polar regions. From these plots a pattern could be recognized. It was obvious that the light reflected by Earth had a large dependency on the latitude, but only a small on longitude. Figure 6 shows an example of the reflectivity of Earth as a function of its latitude. The solid curve is the average reflectivity and the dashed the standard deviation as a function of the latitude of Earth. The reflectivity has a maximum in the polar regions where the deviations are smallest. This is due to the constant ice or snow coverage. For lower latitudes the reflectivity decreases and the deviations increase, respectively. The deviations are due to local differences in the reflectivity of the surface but also due to tidal changes of, for example, cloud formations which have a high reflectivity.

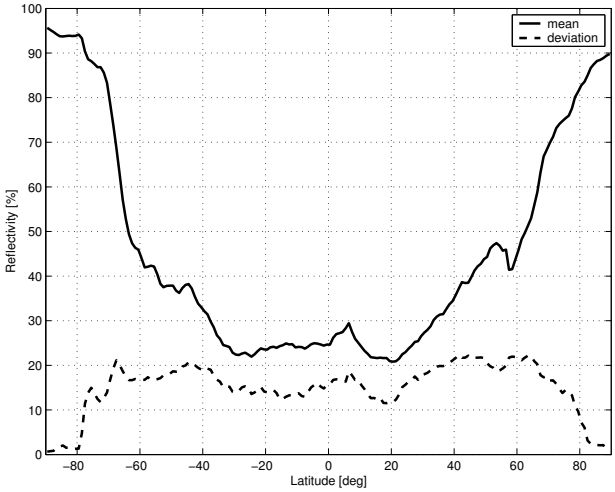

Figure 6: Latitude dependency of the Earth's reflectivity.

Knowing this, a statistical model of the reflectivity can be developed. From the data averages and standard deviations are derived for each latitude. The reflectivity model is created by randomizing new reflectivities based on these averages and deviations for each latitude. The data is merged in order to generate a model of the whole surface of the Earth. This reflectivity pattern is applied to the numerical model of Earth.

Computing the Albedo Light Vector

As the light reflected by Earth is emitted diffusely the cosine law is applicable to calculate the received light by the satellite in any position above the Earth surface. It will suffice to calculate under which angle each surface element is illuminated by the Sun and from which angle it is seen by the satellite. The vector towards Sun is known and so is also the position of the satellite. For each element a normal is calculated as is also the vector pointing towards the satellite. The vector products between the Sun vector and the surface normal as well as between the surface normal and the satellite vector are calculated respectively. Both products are multiplied with each other and the reflectivity of the element. This is the numerical solution to Equation 3 and the solution can now be calculated for every position.
A shell describing a grid of satellite locations at a certain altitude above the Earth surface is created. In every grid point the elements that are visible from the satellite and are illuminated by the Sun are picked out. For the elements surviving the test the emitted albedo light vector is calculated using the cosine law as described above. Now the sum of the contributions from all elements is calculated for each satellite point in the grid, see figure 7, where

$$\underline{I}_{total} = \sum_{k=1}^{n} \underline{I}_k \tag{4}$$

$\underline{I}_total$	Total albedo light vector.
$\underline{I}_k$	Albedo light vector of Earth surface element k.

This total albedo light vector is split up into three components, north, east and down. This coordinate system is chosen to make the curve fitting to come easier, that is, to avoid sine and cosine patterns from the transformation to occur in the plots.

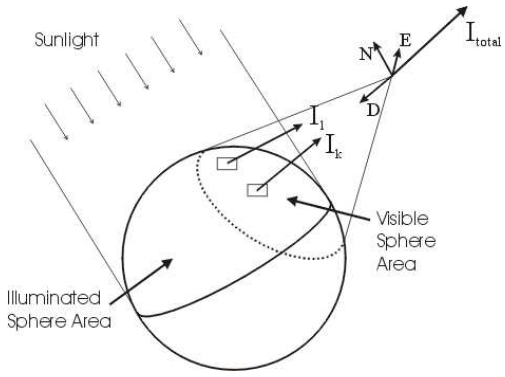

Figure 7: Computing the albedo light vector at satellite position.

With knowledge of the attitude of the satellite having its solar cells in this position this would be the numerical representation of Equation 3. The attitude is not taken into calculation at this moment.
The above procedure is run through several times, each time with a new randomized reflectivity applied to the numerical Earth and for all satellite positions. The mean received albedo intensity of the three components is recorded as well as the standard deviations for every

run. This results in three matrices describing the mean of the albedo light vector in the three components and three matrices describing their deviations w.r.t. the satellite position.

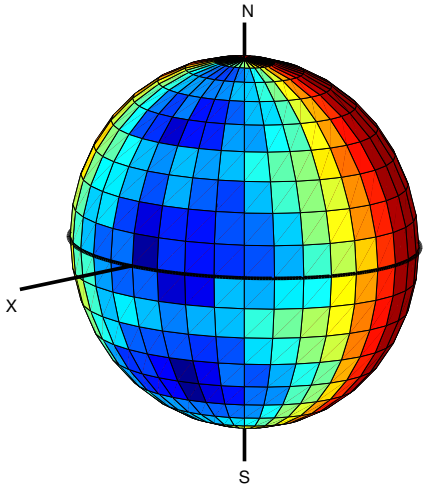

Figure 8: Mean albedo light intensity in down-direction scaled by the sunlight intensity, Sun vector is $[1,\ 0,\ 0]$.

Figure 8 shows a result from these simulations. It describes the down component of the albedo light vector. The intensity on the z-axis is normalized w.r.t. the solar intensity. These six data sets are only valid for this altitude and for this Sun position. For other setups new data sets have to be developed.

Look-Up Tables or Functions

As stated above the look-up tables are only valid for a certain altitude and a certain position of the Sun. For a satellite that stays a long time in orbit and/or has an eccentric orbit this means a lot of data sets and so a lot of memory capacity needed. One solution is to transfer the look-up tables into functions with fewer parameters instead. Functions are very memory saving as they only need to include the functions themselves and a corresponding parameter vector for the current setup.
So the six two-dimensional data arrays describing the incoming light are fitted with two-dimensional functions of the latitude and the longitude with the structure where I is the intensity received by the satellite, $f(latitude)$ is a function describing the dependency on the latitude and $g(longitude)$ a function describing the dependency on longitude. A, B, C and D are scalars that are used to fit the data.
In order to simplify the fitting the coordinates of the data are transferred to a converted longitude and latitude. The longitude is defined between the dawn and dusk meridian (0 to 180 deg) The zero latitude is at the North Pole; hence the plots show the latitudes beginning from the shadow side of Earth, sweeping over the North Pole, the South Pole and back to the shadow side (see figure 9).

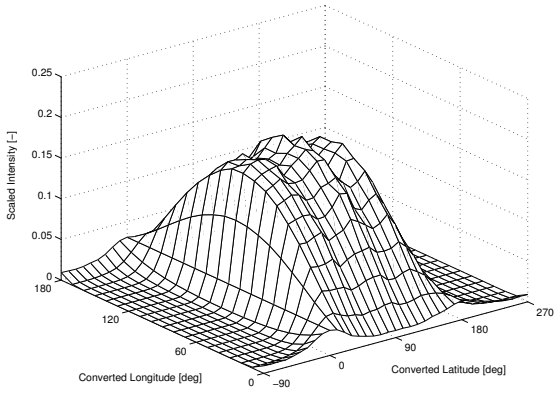

Figure 9: Data plot of mean albedo light intensity in down-direction scaled by the sunlight intensity, sun vector is $[1,\ 0,\ 0]$ (converted coordinates).

The result of the curve fitting can be seen in figure 10. The fitted model represents the down component. The plot is the fitted model to figure 9. The parameter vector creating this plot is saved and later used in the Kalman Filter and for simulating the CSS.

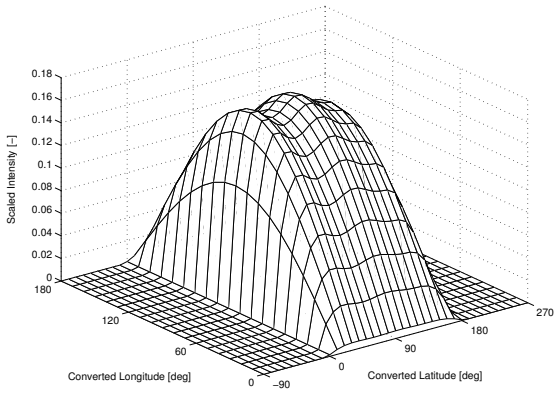

Figure 10: Function fitted to data of mean albedo light intensity (see figure 9), Sun vector is $[1,\ 0,\ 0]$ (converted coordinates).

The functions are used to describe the albedo intensity and the standard deviation, received by the satellite for an arbitrary position in the orbit. The mean parts of the polynomials are used in the Kalman Filter as expected measurements as they deliver the solution to Equation 3 for all positions. All functions together are used to simulate measurements when testing the filter as described later.

Kalman Filter for Attitude Estimation

In order to apply the albedo model derived in the section above an Extended Kalman Filter is applied to estimate the state of a satellite using a Coarse Sun Sensor and a magnetometer.

State Vector and Dynamics Model

The state vector of the Kalman Filter is composed of the rotation rates defined in the body fixed frame and the quaternions describing the spacecraft attitude w.r.t. the inertial frame

$$\underline{x}\,(t) = (\omega_x, \omega_y, \omega_z, q_1, q_2, q_3, q_4)^T \tag{5}$$

where $\underline{\omega}$ is the rotation rate vector and $\underline{q}$ the quaternion vector.
As the dynamic model for the Kalman Filter the rigid body dynamics are applied

$$\dot{\underline{\omega}} = \underline{\underline{I}}^{-1}[\underline{T}_{control}\underline{T}_{dist} - \underline{\omega} \times \underline{\underline{I}}\,\underline{\omega}] \tag{6}$$

$$\dot{\underline{q}} = \frac{1}{2}\tilde{\underline{\omega}} \otimes \underline{q} \tag{7}$$

where $\underline{\underline{I}}$ is the inertia matrix of the spacecraft. The vector $\underline{T}_{control}$ comprises all control torques produced by the attitude control system. The vector $\underline{T}_{dist}$ includes all external disturbance torques acting on the satellite. The disturbance torques taken into account are those from the gravity gradient, magnetic and aerodynamic drag and solar pressure.
For an Extended Continuous Discrete Kalman Filter the system matrix $\underline{\underline{F}}$ is needed which is defined as the partial derivatives of the equation of motion w.r.t. the state vector

$$\underline{\underline{F}} = \frac{\partial \dot{\underline{x}}}{\partial \underline{x}}. \tag{8}$$

In this case the resulting matrix $\underline{\underline{F}}$ is a 7 by 7 element matrix.

Measurement Model and Observation Matrix

The observation vector consists of the measurements from the six solar cells and the vector measurement from the magnetometer. It is defined as

$$\underline{h}^T = \left[\underline{h}_{CSS}^T, \underline{h}_{Mag}^T\right]. \tag{9}$$

The measurement model for the Sun sensor is a combination of six measured voltages. Each voltage is obtained from the current of the solar cells via a resistor. The observation vector for the CSS can be written as

$$\underline{h}_{CSS} = [U_{+X}, U_{-X}, U_{+Y}, U_{-Y}, U_{+Z}, U_{-Z}]^T \tag{10}$$

where U_i is the measured voltage for the solar cell in the direction i. Each voltage can be obtained from the following attitude dependent equation

$$U_i = U_{Sun,\perp}\Big(g\left\{\underline{e}_i^{b\,T} \cdot \underline{\underline{A}}_i^b\left(\underline{q}\right) \cdot \underline{P}_{sun}^i\right\} + g\left\{\underline{e}_i^{b\,T} \cdot \underline{\underline{A}}_i^b\left(\underline{q}\right) \cdot \underline{P}_{albedo}^i\right\}\Big) \tag{11}$$

where

$U_{Sun,\perp}$	Voltage delivered for perpendicular sunlight incident.
$\underline{P}_{sun}^i$	Sunlight vector in inertial frame.
$\underline{P}_{albedo}^i$	Albedo light vector in inertial frame.
$\underline{\underline{A}}_i^b\left(\underline{q}\right)$	Attitude matrix as a function of the attitude quaternion $\underline{q}$.
$\underline{e}_i^b$	Vector normal to the solar cell in the direction i.
$g\{f\}$	Function defined as $g\{f\} = \begin{cases} 0, & f < 0 \\ f, & f \geq 0 \end{cases}$.

The magnetometer observation is defined as

$$\underline{h}_{Mag} = \underline{\underline{A}}_i^b\left(\underline{q}\right) \cdot \underline{B}^i \tag{12}$$

where

$\underline{B}^i$	Magnetic field vector defined in the inertial frame.

The observation matrix needed by the Kalman Filter is defined as the measurement vector $\underline{h}$ partially differentiated w.r.t. the state vector. For this application it is assumed that only the term $\underline{\underline{A}}_i^b\left(\underline{q}\right)$ is dependent on the state.

Improved Measurement Model

The preparation of the algorithm for application in an attitude control system has rendered two improvements to the Kalman Filter.

1. The measurements of the CSS are combined to a single vector showing the direction of the total light vector. It can be computed from the solar cell measurements using equation 1. If we use the equations 10 and 11 we get the CSS measurement as vector of size 3 as

$$\underline{h}_{CSS} = \underline{\underline{A}}_i^b\left(\underline{q}\right) \cdot \left(\underline{P}_{sun}^i + \underline{P}_{albedo}^i\right). \quad (13)$$

   Using this approach the parameter describing the voltage delivered by a solar cell at perpendicular sunlight incident $U_{Sun,\perp}$ can be omitted.

2. The normalized magnetic field vector is used as an observation. It can be written as

$$\underline{h}_{Mag} = \frac{1}{|B|}\underline{\underline{A}}_i^b\left(\underline{q}\right) \cdot \underline{B}^i. \quad (14)$$

   This reduces the influence of the magnitude of the vector on the attitude estimation.

Simulation Results

The Extended Kalman Filter for attitude determination using a Coarse Sun Sensor and a magnetometer developed in the section above is now checked by running simulations. For that purpose the orbit and the attitude of the satellite are simulated using the in-house tool SATSIM.[5] It is a simulation tool developed by the Center of Applied Space Technology and Microgravity (ZARM) to provide a test bench for the development of attitude control systems for small satellites. The SATSIM program simulates the orbital- and attitude dynamics of the satellite including disturbances (magnetic, aerodynamic, radiation pressure) as well as control torques and forces. In the simulations the true state simulated by SATSIM is used to generate measurements as input to the Kalman Filter algorithm. The estimated attitude is compared to the true state.

Scenario Definition

In the simulations a satellite of a cubic shape was used. It has the following properties:

- Size:
$$1\,m \times 1\,m \times 1\,m$$
- Mass:
$$m = 300\,kg$$
- Displacement between geometrical center and center of mass:
$$\underline{r}_{GC,COM} = \begin{bmatrix} 0.1 \\ 0.05 \\ 0.04 \end{bmatrix} m$$
- Moments of inertia
$$\underline{\underline{I}} = \begin{bmatrix} 53 & 1.5 & 1.2 \\ 1.5 & 50.75 & 0.6 \\ 1.2 & 0.6 & 50.48 \end{bmatrix} kg\,m^2$$

In the simulations different orbits are used. They have the following parameters:

- Altitude:
$$h = 630\,km$$
- Eccentricity:
$$\varepsilon = 0.01$$
- Inclination (nominal case / worst case):
$$i = 30\,deg / 90\,deg$$
- Right ascension of ascending node (nominal case / worst case):
$$\Omega = 90\,deg / 0\,deg$$
- Sun position:
$$\underline{e}_{Sun}^i = (1,\, 0,\, 0)$$

The initial attitude of the satellite is arbitrarily chosen with a maximum total rate of $\omega = 0.01\,rad/s$. This can be applied since it is assumed that the detumbling phase of attitude acquisition has already been completed. The Kalman Filter has no a-priori knowledge of the attitude. The initial state of the estimated attitude is set to the following values:

$$\begin{aligned} \underline{\omega} &= (0,\, 0,\, 0)^T \\ \underline{q} &= (0.5,\, 0.5,\, 0.5,\, 0.5)^T \end{aligned} \quad (15)$$

Error Sources and Disturbances

In order to make the simulations more realistic and to prove the robustness of the algorithm some disturbances and errors are included.

1. The Kalman Filter uses information about the dynamics of the satellite. Especially the moments of inertia are a central parameter. In order to check the sensitivity of the algorithm the moments of inertia provided to the Kalman Filter are changed by 5% w.r.t. the real simulated values. This is a reasonable value as small satellites with limited budget may have uncertainties in the mass configuration of the spacecraft. Also the difference in propellant mass, if present and not modeled, over time affects the moments of inertia of the satellite.

2. It is furthermore assumed that the position of the satellite needed for computing the expected measurements of the magnetometer and the CSS can not be precisely determined on board. To simulate this a position error has been introduced. The Kalman Filter is given a position that differs up to $1\,deg$ in latitude and longitude from the true value.

3. The attitude dynamics is influenced by external torques. Those are the gravity gradient, magnetic- and aerodynamic drag and solar pressure. In the simulation of the dynamics using SATSIM they are all included.[5] These torques are not known to the Kalman Filter. The total unknown torque varies between $10^{-5}\,Nm$ and $5 \cdot 10^{-7}\,Nm$ depending on the position and attitude of the satellite.

Measurement and Modeling Noise

Measurements have to be simulated as input to the filter. The magnetic field vector is computed by a function based on the IGRF model.[1] The model is distorted by white noise with a $200\,nT$ amplitude[6] run through a low pass filter to simulate the local and tidal changes. Another white noise with amplitude $2\,nT$ is added to simulate measurement noise. The magnetic field vector delivered to the filter is described in an inertial frame.
The received light is composed of one part coming from the Sun, and another part that has been reflected by Earth. The latter part is created using the functions for the mean light vector as a base. A random number with a position dependent standard deviation is added. This number is derived from those functions of the albedo model describing the uncertainty of the reflected light. The result is put through a low pass filter to simulate the low frequencies at which the albedo measurements can be assumed to change. The light vectors are added and split up into six non-negative scalars representing the voltages measured for each of the solar cells on all sides of the satellite. To these scalars a white, unfiltered noise with amplitude 0.5% of the measured intensity is added before they are given to the filter as measurements. This reflects the electronics noise of the analog digital converter.

Filter Tuning

Subject to the filter tuning are the settings for the measurement noise covariance matrix $\underline{\underline{R}}$ and the system noise covariance matrix $\underline{\underline{Q}}$. In the latter case the values are selected that the uncertainties concerning the external disturbance torques are considered. The measurement noise covariance matrix is set to values which reflect the expected accuracy of the sensors.

Nominal Case

In figure 11 the results for the nominal case are shown. The plot A describes the intensity of the reflected light, normalized w.r.t. the solar intensity in the NED frame. The curve with the largest amplitude is the down component, the second greatest the north component and the weakest is the east component of the incoming vector. This intensity distribution is natural as the satellite in this case is passing right over the most radiating part of Earth, that is, the part receiving the most sunlight.
The plot B shows the modeled standard deviations for the Earth albedo light vector. They are also expressed in the NED-frame and are normalized w.r.t. the sunlight intensity. It can be seen that the largest deviations are present in the down component. This is expected as this component is the largest. The deviations are up to $10\,\%$ of the albedo radiation. The two other components are similar in size and partially also larger than the mean values they correspond to. This has the consequence that the mean values should be trusted poorly.

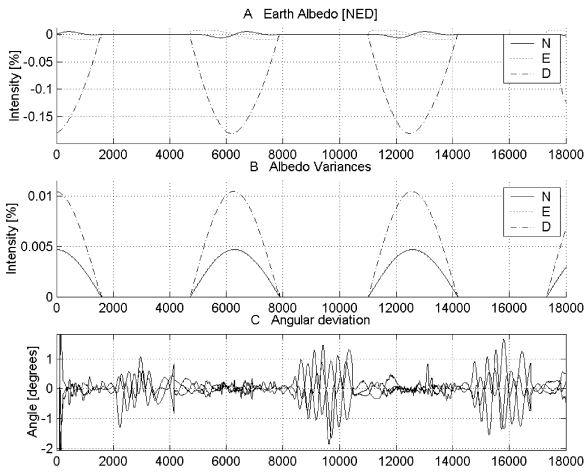

Figure 11: Results for nominal case: (A) Albedo light; (B) Albedo deviation; (C) Attitude estimation error

The plot C shows the attitude estimation error of the angles around all three body-fixed axes in degrees. The plot shows clearly the shadow phases where the magnetometer only is used for attitude determination. After reacquiring the Sun the accuracy improves from $1.5\,deg$ in the shadow to less than $0.5\,deg$. The accuracy in the shadow phase is mainly determined by the accuracy of the dynamic model used in the Kalman Filter. Since this is inaccurate due to unknown disturbances, a position error and an uncertainty in the moments of inertia the relatively large deviations of about $1.5\,deg$ can be explained.

Observability Issues

The Kalman Filter uses the information from the sensors to create two vectors. Using these vectors the filter is able to determine the full attitude of the satellite. This is only possible if the two vectors are both present and are not pointing in the same direction. For a nearly polar orbit this issue can occur.

Figure 12 shows a polar orbit. In this case the magnetic field vector is close to parallel to the orbital plane. If the Sun vector is also close to the orbital plane both vector observations become parallel and the observability of the attitude becomes poor. This can be expressed by the absolute value of the angle between the two vectors.

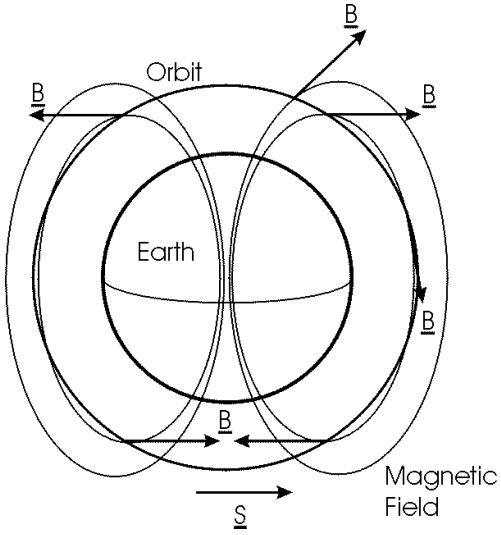

Figure 12: Geometry for occurrence of a small angle between two vector observations $\underline{B}$ (magnetic field) and $\underline{S}$ (sun vector).

A measure for the angle between the two vectors is the dot product or cosine of the angle between the vectors

$$\cos(\alpha) = \underline{B} \circ \underline{S}. \tag{16}$$

If this value is close to zero the angle between the vectors is small and the observability is poor. For these cases a poor attitude estimation can be expected.

Figure 13 shows in plot C the attitude estimation error for a polar orbit with an orbital plane close to parallel to the Sun vector. The plot shows several peaks (e.g. at $800\,s$, $6000\,s$, $7000\,s$) of an increased estimation error. These peaks coincide with situations of poor observability which can be seen in plot D. It shows the cosine of the angle between the two vectors as expressed in equation 16.

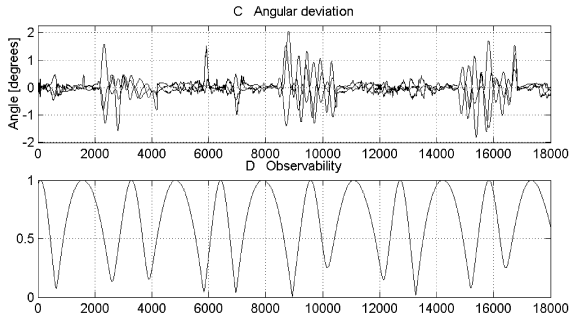

Figure 13: Results for polar orbit with observability issues: (C) Attitude estimation error; (D) Observability measure

The knowledge of the observability can be used for compensation. Every time the two vectors become close to parallel the observability is poor or, expressed in other words, the observations have to be weighted less. This can be achieved by introducing a tuning factor for the measurement noise covariance matrix $\underline{\underline{R}}$. It is increased for a poor observability which has the effect that the Kalman Filter relies more on the system dynamics than on the measurements. Using this approach the estimation could be improved as it is shown in figure 14. The plot E shows the tuning factor for the matrix $\underline{\underline{R}}$. It is increased when the observability measure drops below 0.5.

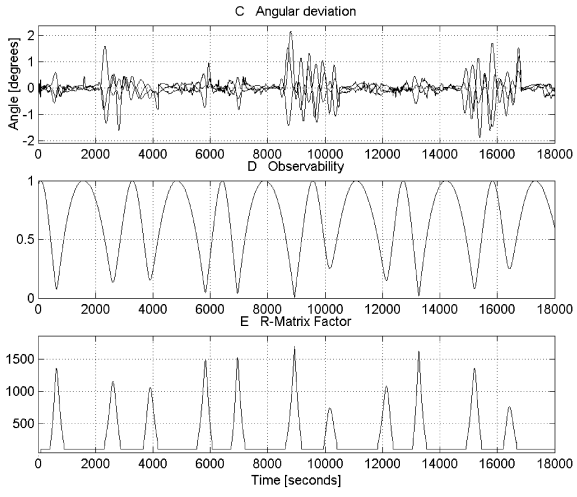

Figure 14: Results for polar orbit with compensation for observability issues: (C) Attitude estimation error; (D) Observability measure; (E) Tuning factor for the observation matrix $\underline{\underline{R}}$.

Using this method the peaks of an increased estimation error can be reduced below $1\,deg.$ (compare figure 13 plot C and figure 14 plot C).

Conclusions

This paper has presented a method for using low cost Coarse Sun Sensor and magnetometer to get a good accuracy for attitude determination. The keys for the success of this method are the model of the Earth albedo light and the utilization of state estimation techniques.
In order to use this method for on-board attitude determination the following inputs and parameters are needed:

- The satellite position from orbit propagator needed for the IGRF model as well as for the albedo model,
- the Sun position (Sun vector),
- the albedo model as look-up tables or parametrical functions,
- the magnetic field model (IGRF),
- satellite properties (at least moments of inertia).

The simulations have shown that the attitude estimation algorithm based on an Extended Kalman Filter are robust to:

- unknown disturbance torques (up to $10^{-5}\,Nm$),
- uncertainties in the moments of inertia (5% error),
- errors in position knowledge ($1\,deg$ in latitude and longitude),
- moderate modeling errors and measurement noise.

Despite these issues the algorithm shows a good accuracy of better than 1 degree in all axes for the nominal case. In the case of a polar orbit where the observability gets poor an accuracy of better than 2 degrees can be maintained. The application of the Coarse Sun Sensor for this purpose is sufficient and the costs are much lower than for a fine Sun sensor. The sensor is also reliable because of its simple construction. Due to the fact that this sensor is used for acquisition modes either an additional fine Sun sensor is not necessary. As a complement or substitute to the small sensors the ordinary solar cells of a satellite can be used.
A combination of the Coarse Sun Sensor and magnetometer is simple, robust and accurate for acquisition and safe modes. It provides a sufficient accuracy for nominal modes of most small satellite applications and saves the costs of additional hardware.

References

[1] *International Geomagnetic Reference Field (IGRF)*. http://nssdc.gsfc.nasa.gov-/space/model/models/igrf.html.

[2] *Total Ozone Mapping Spectrometer (TOMS)*. http://toms.gsfc.nasa.gov/.

[3] Arthur Gelb, editor. *Applied Optimal Estimation*. The MIT Press, 1974.

[4] M.S. Grewal and A.P. Andrews. *Kalman Filtering - Theory and Practice*. Prentice Hall, Englewood Cliffs, New Jersey, 1993.

[5] S. Theil, M. Wiegand, and H. J. Rath. SATSIM - A Generic Tool for Attitude Control System Development, Simulation and Testing. In *51st International Astronautical Congress, Rio de Janeiro, Brazil*, October 2000.

[6] M. Wiegand. Autonomous Satellite Navigation via Kalman Filtering of Magnetometer Data. In *46th International Astronautical Congress, Oslo, Norway*. IAF, October 1995.